$\chi_{c1}(4274)$ multiplicity in heavy-ion collisions

L. M. Abreu [*]
Instituto de Física, Universidade Federal da Bahia, Campus Universitário de Ondina, 40170-115 Bahia, Brazil and Instituto de Física, Universidade de São Paulo, Rua do Matão, 1371, CEP 05508-090, São Paulo, Brazil

A. L. M. Britto [†]
Centro de Ciências Exatas e Tecnológicas, Universidade Federal do Recôncavo da Bahia, R. Rui Barbosa, Cruz das Almas, 44380-000 Bahia, Brazil and Instituto de Física, Universidade Federal da Bahia, Campus Universitário de Ondina, 40170-115 Bahia, Brazil

F. S. Navarra [‡]
Instituto de Física, Universidade de São Paulo, Rua do Matão, 1371, CEP 05508-090, São Paulo, Brazil

H. P. L. Vieira
Instituto de Física, Universidade Federal da Bahia, Campus Universitário de Ondina, 40170-115 Bahia, Brazil

(Received 13 October 2023; accepted 16 January 2024; published 31 January 2024)

In a previous work we computed the thermally averaged cross sections for the production and absorption reactions of the $\chi_{c1}(4274)$ state in the hot hadron gas formed in heavy-ion collisions. In the present work we estimate the final yield of the $\chi_{c1}(4274)$ state in these collisions. We use the coalescence model to fix the initial multiplicity of the $\chi_{c1}(4274)$, which is treated as a P-wave bound state of $D_s\bar{D}_{s0}$ and also as a compact tetraquark. The Bjorken picture is used to model the hydrodynamic expansion and cooling. We also consider the Hubble cooling, which is faster and mimics the effect of the transverse expansion. Then, the kinetic equation is solved to evaluate the time evolution of the $\chi_{c1}(4274)$ yield during the hot hadron gas phase. Since the $\chi_{c1}(4274)$ decay width is large it might decay inside the hadron gas. Therefore, we also include the $\chi_{c1}(4274)$ decay and regeneration terms by means of an effective coupling, estimated from the available data. The combined effects of hadronic interactions and the $\chi_{c1}(4274)$ decay have a strong impact on the final yield. Also, predictions of the $\chi_{c1}(4274)$ multiplicity as a function of centrality and of the charged hadron multiplicity measured at midrapidity $[dN_{ch}/d\eta(\eta < 0.5)]$ are presented. Finally, we calculate the yield of a proposed P-wave molecular state of $D_s\bar{D}_{s0}$, $Y'(4274)$, characterized by a smaller width and smaller coupling constant obtained from the Weinberg compositeness condition.

DOI: 10.1103/PhysRevD.109.014041

I. INTRODUCTION

During the last two decades, the number of new hadrons has increased substantially [1], with the observation of new states whose properties are incompatible with the quark model predictions. One of these unconventional structures with very intriguing properties is the charmoniumlike $\chi_{c1}(4274)$ state. It has been observed by the LHCb Collaboration in the amplitude analysis of the decay $B^+ \to J/\psi\phi K^+$. Its quantum numbers have been established to be $I^G(J^{PC}) = 0^+(1^{++})$ with statistical significance of 6.0σ, and its corresponding measured mass and width are [2,3]

$$M_\chi = 4273.3 \pm 8.3^{+17.2}_{-3.6}\ \text{MeV}, \quad \Gamma_\chi = 56 \pm 11^{+8.0}_{-11}\ \text{MeV}, \quad (1)$$

at 5.8σ of significance. These values of mass and width are consistent with a previous measurement claimed by the CDF Collaboration [4]:

[*] luciano.abreu@ufba.br
[†] andrebritto@ufrb.edu.br
[‡] navarra@if.usp.br

$$M_\chi = 4274.4^{+8.4}_{-6.7}\ \text{MeV}, \qquad \Gamma_\chi = 32.3^{+21.9}_{-15.3}\ \text{MeV}. \tag{2}$$

Several works were dedicated to understand the properties and intrinsic nature of the $\chi_{c1}(4274)$ [5–14]. There were attempts to interpret $\chi_{c1}(4274)$ as a S-wave $cs\bar{s}\,\bar{c}$ tetraquark state, as a conventional $\chi_{c1}(3^3P_1)$ structure, as a color triplet and sextet diquark-antidiquark configuration, as a molecular state of mesons, and others (we refer the reader to Ref. [15] for a more detailed discussion).

Motivated by the fact that the $\chi_{c1}(4274)$ mass is just 12 MeV below the $D_s\bar{D}_{s0}(2317)$ threshold, the author of Ref. [13] has performed an analysis of the $\chi_{c1}(4274)$ as a P-wave bound state of $D_sD_{s0}(2317)$ in a quasipotential Bethe-Salpeter equation approach, with a partial wave decomposition on spin parity. The quantum numbers of D_s and $\bar{D}_{s0}(2317)$ (denoted from now on by $\bar{D}_{s0}$) are 0^- and 0^+ and hence the binding mechanism between these two mesons must be in P-wave and strong enough to generate a bound state. However, this idea was not supported by the results found in Ref. [14], where calculations based on an effective approach with the Weinberg compositeness condition gave a much smaller partial decay width for the $\chi_{c1}(4274)$ than the one experimentally observed. In view of these results the authors of Ref. [14] proposed the existence of a new D_sD_{s0} P-wave bound state called $Y'(4274)$.

The debate on the properties of the $\chi_{c1}(4274)$ will continue and certainly there will be more contributions on this issue. From the experimental side, heavy-ion collisions (HICs) appear as a promising scenario to investigate the properties of exotic states, as was pointed out in previous works [16–21]. The final $\chi_{c1}(4274)$ multiplicity will depend on the interaction cross sections, which, in turn, depend on the spatial configuration of the quarks. Meson molecules are larger, and therefore have greater cross sections, which means that they will have a stronger interaction with the hadronic medium than compact tetraquarks. In Ref. [15] we studied the interactions of the $\chi_{c1}(4274)$ with a hadronic medium via an effective approach, and we found significant differences between the thermally averaged cross sections for the $\chi_{c1}(4274)$ production and suppression reactions. These findings motivate us to pursue this investigation and use the obtained thermal cross sections to estimate the final yield of the $\chi_{c1}(4274)$ in a heavy-ion collision environment. We use the coalescence model to fix the initial multiplicity of the $\chi_{c1}(4274)$, which is treated as a P-wave bound state of $D_s\bar{D}_{s0}$ and also as a compact tetraquark. The hydrodynamic expansion is described by the Bjorken model. With these inputs we solve the kinetic equation to determine the time evolution of the $\chi_{c1}(4274)$ yield during the hot hadron gas phase. Finally we present predictions for the $\chi_{c1}(4274)$ multiplicity as a function of centrality and charged hadron multiplicity measured at midrapidity $[dN_{ch}/d\eta(\eta < 0.5)]$. Additionally, we compute the yield of the P-wave molecular state of $D_s\bar{D}_{s0}$, $Y'(4274)$ proposed in Ref. [14].

This work is organized as follows. In the next section, we present the formalism; the rate equation that drives the time evolution of the χ_{c1} abundance, the coalescence model and how the dependence with centrality and charged hadron multiplicity measured at midrapidity is implemented. Section III is devoted to discuss the results and in the last section we present the concluding remarks.

II. FORMALISM

A. Kinetic equation

In order to estimate the time evolution of the χ_{c1} yield we employ the integrodifferential equation given by [16–21]

$$\begin{aligned}\frac{dN_\chi(\tau)}{d\tau} = \sum_{\substack{c,c'=D_sD_{s0}\\ a=\pi,K,\eta,\\ \rho,K^*,\omega}} &[\langle\sigma_{cc'\to\chi a}v_{cc'}\rangle n_c(\tau)N_{c'}(\tau)\\ &-\langle\sigma_{\chi a\to cc'}v_{\chi a}\rangle n_\phi(\tau)N_\chi(\tau)]\\ &+\langle\sigma_{J/\psi\phi\to Y}v_{J/\psi\phi}\rangle n_\phi(\tau)N_{J/\psi}(\tau)\\ &-\Gamma_{\chi_{c1}}N_\chi(\tau),\end{aligned} \tag{3}$$

where $N_\chi(\tau)$ and $N_{c'}(\tau)$ represent the abundance of χ_{c1} and the charmed (strange) mesons at proper time τ; $n_c(\tau)$, and $n_\phi(\tau)$ are the number densities of charmed strange mesons and light mesons, respectively. We assume that the hadron gas is in thermal equilibrium, and its constituents have their respective densities following the Boltzmann distribution, i.e.,

$$n_i = \frac{1}{2\pi^2}\gamma_i g_i m_i^2 T(\tau) K_2\left(\frac{m_i}{T(\tau)}\right), \tag{4}$$

with γ_i, g_i, and m_i being the fugacity, degeneracy and mass of the particle i, respectively; $T(\tau)$ is the time-dependent temperature. The multiplicity, $N_i(\tau)$, is obtained by multiplying the abundance, $n_i(\tau)$, by the volume $V(\tau)$.

In Eq. (3), $\langle\sigma_{i\to\chi f}v_i\rangle$ are the thermally averaged cross section calculated and discussed in Ref. [15].

The decay width of χ_{c1} ($\Gamma_{\chi_{c1}}$) is relatively large and its lifetime may be shorter than the lifetime of the hadron gas phase assumed in this work (of the order of 10 fm/c). Therefore, the decay of χ_{c1} as well as its regeneration from the daughter particles of the possible processes are included in the last two lines of Eq. (3). According to [22], only the reaction $\chi_{c1}\to J/\psi\phi$ has been seen, and hence only this one is considered here to estimate the mentioned decay and regeneration terms. We will proceed as in Refs. [23,24]. The decay width $\Gamma_{\chi_{c1}}$ is determined with the help of the effective Lagrangian

$$\mathcal{L} = g_{\chi_{c1}J/\psi\phi}\epsilon_{\mu\nu\rho\sigma}\phi^\mu\psi^\nu(\partial^\rho\chi^\sigma - \partial^\sigma\chi^\rho), \tag{5}$$

with the coupling constant $g_{\chi_{c1}J/\psi\phi}$ being fixed by fitting the experimental data from [2,3]. The decay rate can be written as

$$\Gamma_{\chi_{c1}}(\sqrt{s}) = \frac{p_{cm}(\sqrt{s})}{8\pi s g_\chi}|\mathcal{M}|^2, \tag{6}$$

where p_{cm} is the three-momentum in the center-of-mass frame; $\mathcal{M}$ is the tree-level amplitude of the decay rate expressed by

$$M = g_{\chi_{c1}J/\psi\phi}\epsilon^{\mu\nu\rho\sigma}\varepsilon^*_\mu(p_2)\varepsilon^*_\nu(p_3)[p_{1_\rho}\varepsilon_\sigma(p_1) - p_{1_\sigma}\varepsilon_\rho(p_1)], \tag{7}$$

with the momenta of the states χ_{c1}, J/ψ and ϕ being given by p_1, p_2, and p_3, respectively. The polarization vector is given by $\varepsilon(p)$. Thus, using the experimental value of the χ_{c1}-decay width in Eq. (1), we fix the value of the coupling constant as $g_{\chi_{c1}J/\psi\phi} = 0.56 \pm 0.07$.

Also, the cross section for the regeneration process is assumed to be given by the spin-averaged relativistic Breit-Wigner approximation,

$$\sigma(\sqrt{s}) = \frac{g_\chi}{g_\psi g_\phi}\frac{4\pi}{p^2_{cm}}\frac{s\Gamma^2_{\chi_{c1}}(\sqrt{s})}{(s-M^2_\chi)+s\Gamma^2_{\chi_{c1}}(\sqrt{s})}, \tag{8}$$

where g_χ, g_ψ, and g_ϕ are the degeneracy of the χ_{c1}, J/ψ, and ϕ, respectively. The thermally averaged cross section, $\langle\sigma_{J/\psi\phi\to\chi}v_{J/\psi}\rangle$, is therefore calculated in the same way as done in [15]. Additionally, since the decay width Γ averaged over the thermal distribution does not present a strong dependence on the temperature, we use its value in the vacuum.

Finally, it is worth noticing that the coupling constant $g_{\chi D_s D_{s0}}$ has been determined theoretically in Ref. [14] by means of the Weinberg compositeness condition [25,26], assuming χ_{c1} as a P-wave molecular state of $D_s\bar{D}_{s0}$. With this formalism the predicted decay width is $\Gamma^{(\mathrm{Theo})}_{\chi_{c1}} \sim 1.46$ MeV, much smaller than the experimental one $[\Gamma^{(\mathrm{Exp})}_{\chi_{c1}}]$ given in Eq. (1). This point has been used by the authors of [14] to argue that the molecular interpretation of χ_{c1} is disfavored, as well as to suggest that it would be possible to observe a P-wave molecular state of $D_s\bar{D}_{s0}$ [so-called $Y'(4274)$] at Belle or Belle II experiments. We employ here a different strategy; in order to obtain predictions for observables of our interest based on existing experimental data, we assume that relevant contributions for the observed $\Gamma_{\chi_{c1}}$ are effectively encoded in the coupling $g_{\chi_{c1}J/\psi\phi}$, discussed above from Eq. (5) on, and that the mechanisms involving the coupling among χ_{c1}, D_s, and D_{s0} have a relevant participation. In this sense, we remark that the reaction $\chi_{c1} \to J/\psi\phi$ was evaluated in Ref. [14] from the triangular diagrams $\chi_{c1} \to D_s D_{s0}(\to J/\psi D^\star_s) \to J/\psi\phi$ and $\chi_{c1} \to D_s D_{s0}(\to \phi D^\star_s) \to \phi J/\psi$. Then, the decay rate coming from these diagrams is proportional to $g^2_{\chi D_s D_{s0}}$ while the $\Gamma_{\chi_{c1}}$ calculated through Eq. (6) is proportional to $g^2_{\chi_{c1}J/\psi\phi}$. Therefore, to reproduce the experimental decay width we use the prescription,

$$g_{\chi D_s D_{s0}} \to \tilde{g}_{\chi D_s D_{s0}} = \sqrt{A}g_{\chi D_s D_{s0}}, \tag{9}$$

where $A = \Gamma^{(\mathrm{Exp})}_{\chi_{c1}}/\Gamma^{(\mathrm{Theo})}_{\chi_{c1}}$. This might be interpreted as follows. A factor $\sqrt{A}$ with the rate between the effective coupling estimated via Eq. (6) and the theoretical coupling constant $g_{\chi D_s D_{s0}}$ is introduced in χ, D_s, D_{s0} coupling to make the theoretical prediction in accordance with data. Then, using the values for $\Gamma^{(\mathrm{Exp})}_{\chi_{c1}}$, $\Gamma^{(\mathrm{Theo})}_{\chi_{c1}}$, and $g_{\chi D_s D_{s0}}$ in [14,15], we get $\tilde{g}_{\chi D_s D_{s0}} = 81 \pm 16$. Hence, unless otherwise stated, in the calculations we use the thermally averaged cross sections defined in Ref. [15], but replacing $g_{\chi D_s D_{s0}}$ according to Eq. (9). This produces an increase in the magnitude of the thermally averaged cross sections without qualitative modifications. Another consequence, at a more profound level, is that this prescription makes the nature of the coupling used here independent of a particular interpretation, since it no longer obeys the Weinberg compositeness condition. The intrinsic nature of the χ_{c1} state will be given by the initial condition employed (see discussion in a subsequent subsection).

B. Hydrodynamic expansion

The hadron gas evolution is modeled by the boost invariant Bjorken picture with an accelerated transverse expansion, in which the volume and temperature as a function of the proper time τ are as follows [16,17,20,21]:

$$V(\tau) = \pi\left[R_C + v_C(\tau-\tau_C) + \frac{a_C}{2}(\tau-\tau_C)^2\right]^2 c\tau,$$
$$T(\tau) = T_C - (T_H - T_F)\left(\frac{\tau-\tau_H}{\tau_F-\tau_H}\right)^{\frac{4}{5}}, \tag{10}$$

where R_C, v_C, a_C, and T_C denote the transverse size, transverse velocity, transverse acceleration and temperature at the chemical freeze-out time τ_C, respectively; $T_H(T_F)$ is the temperature at the end of the mixed phase (kinetic freeze-out) time $\tau_H(\tau_F)$. The parameters in Eq. (10) are fixed according to Ref. [27], for a hadronic medium formed in central Pb-Pb collisions at $\sqrt{s_{NN}} = 5.02$ TeV, and the set of parameters is given in Table I.

In addition, in Table I the multiplicities of the light mesons and quarks in charmed mesons are also shown. In the case of light mesons, the fugacities in Eq. (4) are normalization parameters to adjust the multiplicities given in Table I. On the other hand, since the charm quarks are produced in the early stages of the collision, the total number of charm quarks (N_c) in charmed hadrons is

TABLE I. In the first three lines we list the parameters used in Eq. (10) for the hydrodynamic expansion of the hadronic medium produced in central Pb-Pb collisions at $\sqrt{s_{NN}} = 5.02$ TeV [27]. In the next three lines we list the multiplicities of the mesons used in the model. In the last two lines we show the quark masses and multiplicities, and the frequency used in the coalescence model.

v_C (c)	a_C (c^2/fm)	R_C (fm)
0.93	0.005	10.37
τ_C (fm/c)	τ_H (fm/c)	τ_F (fm/c)
7.1	10.2	21.5
T_C (MeV)	T_H (MeV)	T_F (MeV)
156	156	115
$N_\pi(\tau_H)$	$N_K(\tau_H)$	$N_\eta(\tau_H)$
713	133	53
$N_\rho(\tau_H)$	$N_\omega(\tau_H)$	$N_{K^*}(\tau_H)$
183	53	61
N_{D_s}	$N_{D_{s0}}$	
1.31	0.18	
m_c [MeV]	m_s [MeV]	m_q [MeV]
1500	500	350
N_c	N_s	ω_c [MeV]
14	386	220

assumed to be approximately conserved during the hydrodynamic expansion, i.e., $N_c = n_c(\tau) \times V(\tau) = \mathrm{const}$ and this implies a time-dependent charm-quark fugacity factor $\gamma_c \equiv \gamma_c(\tau)$.

C. Initial conditions

As the rate equation (3) describes the time evolution of the yield $\chi_{c1}(4274)$ from the end of the mixed phase on, we need to fix its initial conditions. To this end, we employ the coalescence model, which determines the multiplicity of the hadronic state by overlapping the density matrix of its constituents with its Wigner function. Accordingly, it encodes information concerning the intrinsic structure of the system, such as angular momentum and the type and number of constituent quarks. Thus, by using the definition of the coalescence model and after some manipulations, the number of $\chi_{c1}(4274)$ at time τ_c can be written as [27]

$$N_{\chi_{c1}} \approx g_\chi \prod_{j=1}^{n} \frac{N}{g_i} \prod_{i=1}^{n-1} \frac{(4\pi\sigma_i^2)^{\frac{3}{2}}}{V(1+2\mu_i T\sigma_i^2)} \times \left[\frac{4\mu_i T\sigma_i^2}{3(1+2\mu_i T\sigma_i^2)}\right]^{l_i}, \tag{11}$$

where g_j and N_j are the degeneracy and number of the jth constituent of the $\chi_{c1}(4274)$, and $\sigma_i = (\mu_i\omega)^{-1/2}$; the parameter ω is the so-called oscillator frequency, assuming that the hadron internal structure is represented by an harmonic oscillator; the reduced mass μ is given by

$$\mu_i^{-1} = m_{i+1}^{-1} + \left(\sum_{j=1}^{i} m_j\right)^{-1}.$$

The angular momentum l_i takes on values of 0 and 1 for S-wave and P-wave, respectively.

In the present approach we explore two possible configurations of the $\chi_{c1}(4274)$; a P-wave bound state of $D_s\bar{D}_{s0}$ and a compact tetraquark $cs\bar{c}\,\bar{s}$. In the case of the P-wave molecular state, $l = 1$ in Eq. (11); the angular frequency is $\omega = 6B$, where $B = m_{D_s} + m_{D_{s0}} - m_{\chi_{c1}}$ is the binding energy (the number of charmed strange mesons is given in Table I). For the compact tetraquark configuration, the frequency, the quark number and masses are summarized also in Table I. Hence, putting all these ingredients in Eq. (11), the initial $\chi_{c1}(4274)$ multiplicity in the molecular and tetraquark configurations are

$$N_{\chi_{c1}}^{(\mathrm{Mol})}(\tau_H) = 2.04 \times 10^{-4}, \quad N_{\chi_{c1}}^{(4q)}(\tau_H) = 7.16 \times 10^{-6}. \tag{12}$$

As expected, $N^{(\mathrm{Mol})}(\tau_H) > N^{(4q)}(\tau_H)$ because a shallow bound state is easier to be formed than a compact tetraquark. In the particular case of χ_{c1}, at the end of mixed phase the coalescence mechanism yields more molecules than tetraquarks by a factor of about 24.

D. System size dependence

The multiplicity $N_{\chi_{c1}}$ can also be expressed as a function of the charged-particle pseudorapidity density at midrapidity, $[dN_{ch}/d\eta(|\eta| < 0.5)]$, which is a measurable quantity, and can be associated to the freeze-out temperature through the empirical formula [16,17,28],

$$T_F = T_{F0}\mathrm{e}^{-b\mathcal{N}}, \tag{13}$$

where $T_{F0} = 132.5$ MeV, $b = 0.02$, and $\mathcal{N} \equiv [dN_{ch}/d\eta(|\eta| < 0.5)]^{1/3}$. We will assume that the hadron gas undergoes a Bjorken cooling given by

$$T_{Bj} = T_h\left(\frac{\tau_h}{\tau}\right)^{1/3}, \tag{14}$$

and also a Hubble cooling given by [29,30]

$$T_{\mathrm{Hu}} = T_h\frac{\tau_h}{\tau}. \tag{15}$$

The freeze-out time τ_F in both types of cooling can be written in terms of $\mathcal{N}$ as [16,17,28]

$$\tau_{F_{\mathrm{Bj}}} = \tau_H \left(\frac{T_H}{T_{F0}}\right)^3 \mathrm{e}^{3b\mathcal{N}}, \qquad \tau_{F_{\mathrm{Hu}}} = \tau_H \left(\frac{T_H}{T_{F0}}\right) \mathrm{e}^{b\mathcal{N}}. \tag{16}$$

The Bjorken cooling is valid for a one-dimensional expansion and the Hubble flow mimics the effects of the transverse expansion. In a previous analysis [28] it was found that the Bjorken flow can account for the data on the K^*/K ratio as a function of $\mathcal{N}$, measured by the ALICE Collaboration, while the Hubble is probably too fast. As it can be seen, $\mathcal{N}$ can be considered as an indirect measurement of the duration of the hadronic phase; a larger system (with a larger mass number A) yields a larger charged-particle pseudorapidity density (bigger $\mathcal{N}$), which in its turn generates a longer hadron phase (bigger τ_F). So, the use of Eq. (16) in Eq. (3) allows us to indirectly estimate the dependence of $N_{\chi_{c1}}$ on the system size.

In addition, following Ref. [16], $\mathcal{N}$ can also be related to other observables like the centrality of the collision. For a Pb-Pb collision, the empirical formula connecting $\mathcal{N}$ with the centrality (denoted as x, in %) the relation is [31]

$$\left.\frac{dN_{\mathrm{ch}}}{d\eta}\right|_{|\eta|<0.5} = 2142.16 - 85.76x + 1.89x^2 - 0.03x^3 + 3.67 \times 10^{-5}x^4 - 2.24 \times 10^{-6}x^5 + 5.25 \times 10^{-9}x^6. \tag{17}$$

III. RESULTS

Now we present and discuss the results obtained by solving the Eq. (3) using the initial conditions given by Eq. (12). In the plots shown below, the bands denote the uncertainties coming from the values of the coupling constants (see the discussion in Sec. II A).

In Fig. 1 we show the time evolution of the $\chi_{c1}(4274)$ multiplicity in the case of molecular configuration, encoded in the initial condition $N_{\chi_{c1}}^{(\mathrm{Mol})}(\tau_H)$ given by Eq. (12). For the sake of comparison, we have included the green and gray bands representing respectively the solutions $N_{\chi_{c1}}^{(\mathrm{Mol})}(\tau)$ of the rate equation (3) without and with the last two lines, which are associated to the inclusion of the χ_{c1} decay rate and regeneration terms. As it can be seen from the green band, the loss terms are dominant with respect to the gain ones, and this leads to a sizable suppression of $N_{\chi_{c1}}^{(\mathrm{Mol})}(\tau)$, which at freeze-out time is about 40% of the initial yield, taking into account the central value. When the decay rate is added, $N_{\chi_{c1}}^{(\mathrm{Mol})}(\tau)$ decreases faster and the final yield is about 15% of the initial one. The solid line shows the evolution of the χ_{c1} multiplicity assuming that the initial condition is given by the thermal statistical value. Interestingly, we observe that when we start from an initial value close to statistical one, the interactions approximately preserve this value until the end of the expansion, i.e., the solid line and the gray band stay close to each other.

Moving on to the compact tetraquark configuration, in Fig. 2 we present the time evolution of the χ_{c1} yield, with the initial condition $N_{\chi_{c1}}^{(4q)}(\tau_H)$ given by Eq. (12); the χ_{c1} decay rate and regeneration terms have been included in the calculations. In this case the behavior of $N_{\chi_{c1}}^{(4q)}(\tau)$ is different; at the beginning of the hadron gas phase, the gain terms dominate and generate an expressive increase of the multiplicity, but as time goes on, the hadron gas expands and cools down, affecting mostly the number and densities of the conventional mesons, and the χ_{c1} production rate becomes smaller, causing a decrease of the abundance. Notwithstanding, at the freeze-out time the χ_{c1} final yield is three times larger than the initial value. The solid line is the same as in Fig. 1 and shows the evolution of

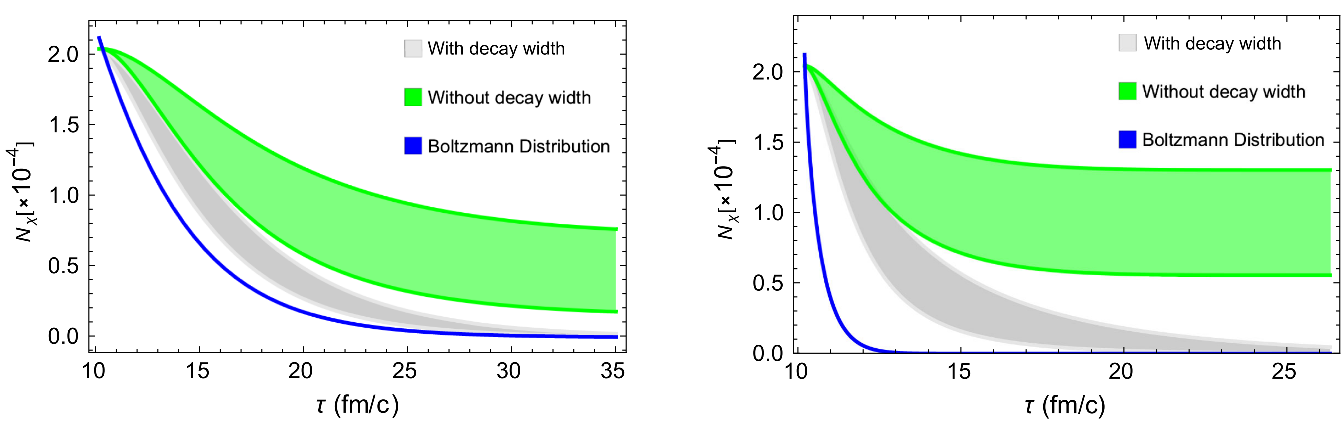

(a) Bjorken cooling

(b) Hubble cooling

FIG. 1. χ_{c1} multiplicity as a function of the proper time in central Pb-Pb collisions at $\sqrt{s_{NN}} = 5.02$ TeV, with initial condition associated to the molecular configuration given by Eq. (12). The solid line shows the evolution of the χ_{c1} multiplicity assuming that the initial condition is given by the thermal statistical value. The time evolution of the temperature is described by the Bjorken cooling (a) and by the Hubble cooling (b).

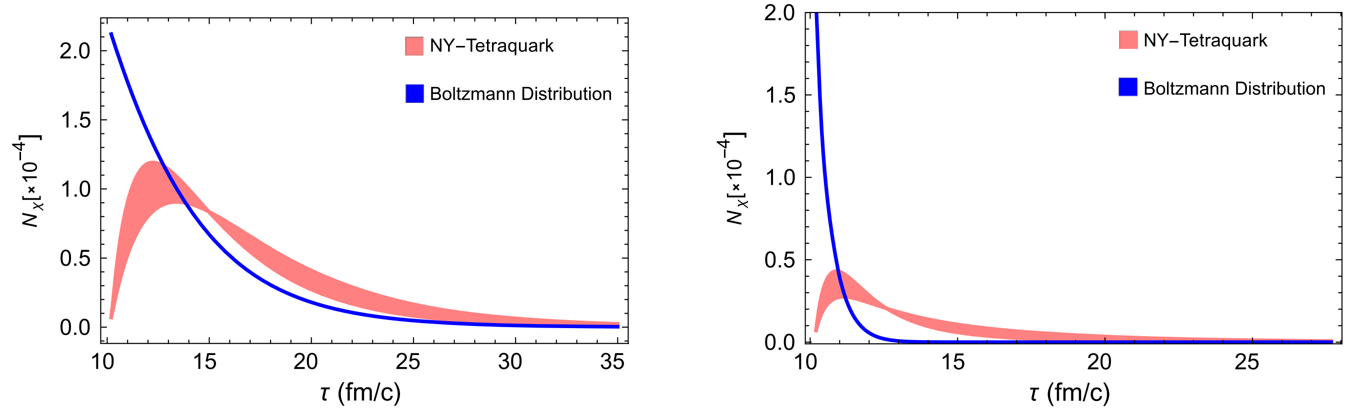

(a) Bjorken cooling (b) Hubble cooling

FIG. 2. χ_{c1} multiplicity as a function of the proper time in central Pb-Pb collisions at $\sqrt{s_{NN}} = 5.02$ TeV, with initial condition associated to the compact tetraquark configuration given by Eq. (12). The solid line shows the evolution of the χ_{c1} multiplicity assuming that the initial condition is given by the thermal statistical value. The time evolution of the temperature is described by the Bjorken cooling (a) and by the Hubble cooling (b).

the χ_{c1} multiplicity assuming that the initial condition is given by the thermal statistical value. As can be seen, at the end of the evolution and after the hadronic interactions, $N_{\chi_{c1}}$ is approximately of the order 3×10^{-5} for both molecular and compact tetraquark configurations and close to the thermal statistical value.

For completeness, we also consider the state $Y'(4274)$ proposed in Ref. [14], assumed there to be a P-wave bound state of $D_s \bar{D}_{s0}$, with a small width and the coupling constant obtained via Weinberg compositeness condition. We use the initial condition $N_{\chi_{c1}}^{(\mathrm{Mol})}(\tau_H)$ given by Eq. (12), and neglect the decay and regeneration terms since the small width implies a decay time which is longer than the duration of the hadron gas phase. In Fig. 3 we plot the $Y'(4274)$ multiplicity as a function of the proper time. The numbers in the figure suggest that the final yield undergoes a small suppression, of the order of 3%, which means that the gain and loss terms in Eq. (3) contribute approximately equally, making the $Y'(4274)$ multiplicity almost constant. As we can see, there is a clear distinction between the predicted molecular state $Y'(4274)$ (obeying the Weinberg compositeness condition) and the χ_{c1} analyzed previously. The final yield of the latter is almost one order of magnitude smaller than that of the former.

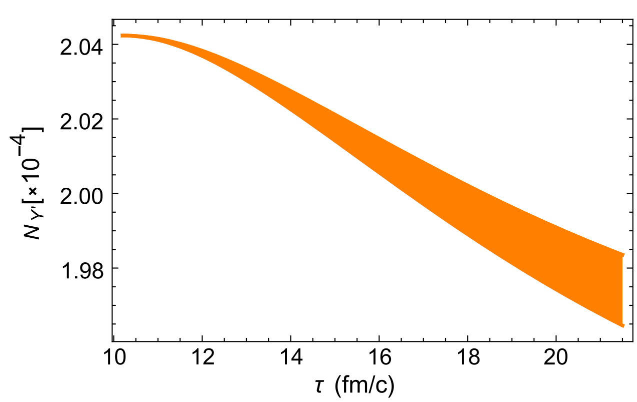

FIG. 3. $Y'(4274)$ multiplicity as a function of the proper time in central Pb-Pb collisions at $\sqrt{s_{NN}} = 5.02$ TeV, with initial condition associated to the molecular interpretation given by Eq. (12).

In Fig. 4 we show the χ_{c1} multiplicity as a function of $\mathcal{N}$. As expected, it grows with the size of the system. Heavy-ion collision experiments can potentially observe a much larger number of χ_{c1}'s (larger systems like Pb-Pb systems are characterized by $\mathcal{N} \sim 10$–12.5) and may provide a very interesting environment for the study of their properties. Curiously, the curves of the molecular and compact tetraquark configurations converge to each other, which suggests that for χ_{c1} the distinction between these configurations is not prominent in larger systems. In this figure we compare the Bjorken cooling, Fig. 4(a), with Hubble cooling, Fig. 4(b). Since the latter is much faster than the former, it preserves more the difference between the multiplicities, which comes from the early times of the hadron gas.

Finally, in Fig. 5 we present the χ_{c1} multiplicity as a function of the centrality, obtained by using Eqs. (16) and (17) in (3). As expected the $\chi_{c1}(4274)$ final yield decreases as we move from central to peripheral collisions. As before the curves for the molecular and compact tetraquark configurations converge to similar values for more central collisions. As in the previous figure, we compare the Bjorken cooling, Fig. 5(a), with Hubble cooling, Fig. 5(b). As before, the latter preserves more the difference between the multiplicities, which comes from the early times of the hadron gas. The smaller systems formed in less central collisions cool faster than larger systems. With the Hubble flow this difference is amplified.

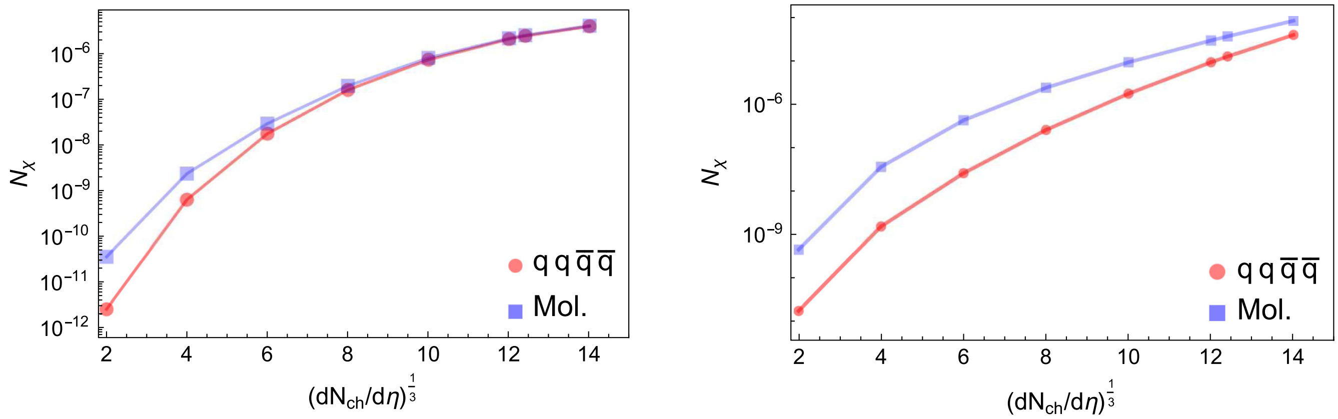

(a) Bjorken cooling (b) Hubble cooling

FIG. 4. χ_{c1} multiplicity as a function of $\mathcal{N}$ for the (a) Bjorken cooling and (b) for Hubble cooling. The curves represent the results obtained with initial conditions associated to the molecular and compact tetraquark configurations given by Eq. (12).

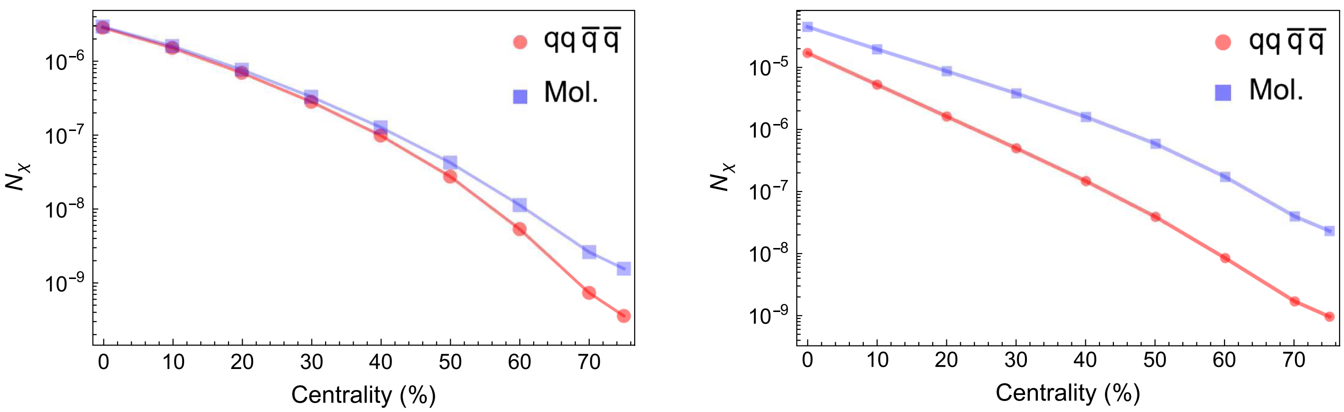

(a) Bjorken cooling (b) Hubble cooling

FIG. 5. χ_{c1} multiplicity as a function of the centrality for the (a) Bjorken cooling and (b) for Hubble cooling. The curves represent the results obtained with initial conditions associated to the molecular and compact tetraquark configurations given by Eq. (12).

Before moving to the conclusions, we would like to emphasize that the Lagrangians are formally the same for tetraquarks and for meson molecules. However the coupling constants are in principle different. In the case of tetraquarks they can be calculated with QCD sum rules [32]. In the case of meson molecules they can be calculated through the evaluation of triangular meson loops with effective theories as done, for example, in [33]. So in principle tetraquarks and molecules have the same Lagrangian but different coupling constants, which can be calculated. However, most of these calculations of couplings have not been done yet. The same considerations apply to the decay widths of tetraquarks and molecules. In the absence of a complete knowledge of couplings and widths, the difference between the two configurations is, in practice, reduced to the difference in the initial conditions. Moreover, the kinetic evolution washes out to a large extent the difference between the tetraquark and molecule multiplicities, a fact that we have observed in all previous calculations involving other exotic states. Finally, we should stress the important role played by smaller systems, where the difference between the tetraquark and molecule multiplicities becomes more evident.

IV. CONCLUDING REMARKS

In this work we have estimated the yield of the $\chi_{c1}(4274)$ state in heavy-ion collisions. In our previous work [15] we found big differences between the thermal cross sections for the production and suppression of $\chi_{c1}(4274)$. Here we have employed them in the rate equation to determine the $N_{\chi_{c1}}$ evolution in time. We have also added the $\chi_{c1}(4274)$ decay and regeneration terms by means of an effective coupling, estimated from the available experimental data, to account for its small lifetime. We have used the coalescence model to compute the initial multiplicity of the $\chi_{c1}(4274)$, which was treated as a P-wave bound state of $D_s\bar{D}_{s0}$ and also as a compact tetraquark. As happened in the case of other multiquark states, meson molecules are much more abundant than tetraquarks. Our results indicate that the combined effects of hadronic interactions, hydrodynamical expansion, and the $\chi_{c1}(4274)$ decay strongly affect the final yield. While for tetraquarks the χ_{c1} yield grows with respect to the initial value, for molecules it decreases. The final number of χ_{c1}'s is approximately equal for both configurations. One can thus conclude that from the multiplicity alone, we cannot determine the intrinsic nature of the $\chi_{c1}(4274)$.

We have also studied the time evolution of the state $Y'(4274)$ proposed in [14] which is characterized by a smaller width and a smaller coupling constant obtained via Weinberg compositeness condition. Our results indicate that the state $Y'(4274)$ has a final yield about one order of magnitude higher than that of the χ_{c1}. Hence, if a vertex detector would be able to accumulate a number of charmed strange mesons as large as 10^4, a small number of $Y'(4274)$ might be observed.

As pointed out in Sec. II, it is important to remark that the nature of the χ_{c1} is encoded in the initial condition, fixed from the coalescence model, which implies a different coalescence mechanism for a hadron molecule and for a compact tetraquark. In the analysis of the hadronic interactions happening during the hadron gas phase, we have employed the same coupling for both scenarios. As a consequence, the larger final yield of the molecular state (as compared to the tetraquark state) for Hubble cooling in Fig. 4 is due to the rapid drop of the statistical limit and a moderate relaxation rate of the molecular state. However, the loosely bound molecular state will favor a larger width, leading to a faster approach to the statistical limit. Thus, the discrepancy between tetraquark and molecular states shown in Fig. 4 could be much smaller. It is also important to mention that using other initial conditions might lead to quite different conclusions. In [34], for example, the authors have considered an opposite initial condition, i.e., larger initial yields of tetraquark state and smaller initial yields of molecular state. The argument supporting this assumption is that a loosely bound molecular state cannot survive in the QGP and thus it almost vanishes before the hadronic stage. They arrive at results which are different from ours. This illustrates the importance of knowing better how these multiquark states are formed. In the future we plan to further study these production mechanisms and also to deepen our study of the coupling constants. This might be done, for example, with the QCD sum rules techniques.

ACKNOWLEDGMENTS

The work of L. M. A. is partly supported by the Brazilian agencies CNPq (Grants No. 309950/2020-1, No. 400215/2022-5, and No. 200567/2022-5), FAPESB (Grant No. INT0007/2016) and CNPq/FAPERJ under the Project INCT-Física Nuclear e Aplicações (Contract No. 464898/2014-5).

[1] For a recent review, see https://qwg.ph.nat.tum.de/exoticshub/.
[2] R. Aaij *et al.* (LHCb Collaboration), Phys. Rev. Lett. **118**, 022003 (2017).
[3] R. Aaij *et al.* (LHCb Collaboration), Phys. Rev. D **95**, 012002 (2017).
[4] T. Aaltonen *et al.* (CDF Collaboration), Mod. Phys. Lett. A **32**, 1750139 (2017).
[5] H. X. Chen, E. L. Cui, W. Chen, X. Liu, and S. L. Zhu, Eur. Phys. J. C **77**, 160 (2017).
[6] Z. G. Wang, Eur. Phys. J. C **77**, 174 (2017).
[7] F. Stancu, J. Phys. G **37**, 075017 (2010); **46**, 019501(E) (2019).
[8] R. Zhu, Phys. Rev. D **94**, 054009 (2016).
[9] Q. F. Lü and Y. B. Dong, Phys. Rev. D **94**, 074007 (2016).
[10] L. C. Gui, L. S. Lu, Q. F. Lü, X. H. Zhong, and Q. Zhao, Phys. Rev. D **98**, 016010 (2018).
[11] S. S. Agaev, K. Azizi, and H. Sundu, Phys. Rev. D **95**, 114003 (2017).
[12] L. Maiani, A. D. Polosa, and V. Riquer, Phys. Rev. D **94**, 054026 (2016).
[13] J. He, Phys. Rev. D **95**, 074004 (2017).
[14] H. Q. Zhu and Y. Huang, Phys. Rev. D **105**, 056011 (2022).
[15] A. L. M. Britto, L. M. Abreu, and F. S. Navarra, Phys. Rev. D **108**, 096028 (2023).
[16] L. M. Abreu, F. S. Navarra, M. Nielsen, and H. P. L. Vieira, Phys. Rev. D **107**, 114013 (2023).
[17] L. M. Abreu, F. S. Navarra, and H. P. L. Vieira, Phys. Rev. D **106**, 074028 (2022).
[18] A. Martinez Torres, K. P. Khemchandani, F. S. Navarra, M. Nielsen, and L. M. Abreu, Phys. Rev. D **90**, 114023 (2014); Acta Phys. Pol. B Proc. Suppl. **8**, 247 (2015).
[19] L. M. Abreu, K. P. Khemchandani, A. Martinez Torres, F. S. Navarra, and M. Nielsen, Phys. Lett. B **761**, 303 (2016).
[20] L. M. Abreu, K. P. Khemchandani, A. Martínez Torres, F. S. Navarra, and M. Nielsen, Phys. Rev. C **97**, 044902 (2018).
[21] L. M. Abreu, F. S. Navarra, and M. Nielsen, Phys. Rev. C **101**, 014906 (2020).
[22] R. L. Workman *et al.* (Particle Data Group), Prog. Theor. Exp. Phys. **2022**, 083C01 (2022).
[23] S. Cho and S. H. Lee, Phys. Rev. C **97**, 034908 (2018).
[24] L. M. Abreu, Phys. Rev. D **103**, 036013 (2021).
[25] S. Weinberg, Phys. Rev. **130**, 776 (1963).
[26] A. Salam, Nuovo Cimento **25**, 224 (1962).

[27] S. Cho *et al.* (ExHIC Collaboration), Prog. Part. Nucl. Phys. **95**, 279 (2017).
[28] C. Le Roux, F. S. Navarra, and L. M. Abreu, Phys. Lett. B **817**, 136284 (2021).
[29] P. Ghosh, J. K. Nayak, S. K. Singh, and S. K. Agarwalla, Phys. Rev. D **101**, 094004 (2020).
[30] S. K. Singh, P. Ghosh, and J. K. Nayak, Phys. Rev. D **104**, 034027 (2021).
[31] H. Niemi, K. J. Eskola, R. Paatelainen, and K. Tuominen, Phys. Rev. C **93**, 014912 (2016).
[32] M. E. Bracco, M. Chiapparini, F. S. Navarra, and M. Nielsen, Prog. Part. Nucl. Phys. **67**, 1019 (2012).
[33] D. Gamermann, J. Nieves, E. Oset, and E. Ruiz Arriola, Phys. Rev. D **81**, 014029 (2010).
[34] B. Wu, X. Du, M. Sibila, and R. Rapp, Eur. Phys. J. A **57**, 122 (2021); **57**, 314(E) (2021).